ACS OMEGA

Open Access

http://pubs.acs.org/journal/acsodf

Article

Redox-Active Conopeptide Li520 Has Evolved to Catalyze Oxidative Folding of Conotoxins

Shweta Dhannura, Shamasoddin Shekh, Pooja Dhurjad, Ashwini Dolle, Sreepriya Kakkat, Vishwajyothi, Marimuthu Vijayasarathy, Rajesh Sonti, and Konkallu Hanumae Gowd*

Cite This: *ACS Omega* 2024, 9, 37596−37609

Read Online

ACCESS | Metrics & More | Article Recommendations | Supporting Information

ABSTRACT: The evolution of miniature conopeptide Li520 (COWC*, *: C-terminal amidation) to exhibit the disulfide isomerase activity was probed using structure, function, disulfide conformation, and the precursor gene sequence. The peptides Li520, Li504, [O2A]Li520, [W3A]Li520, and Grx506, homologues active-site motif of glutaredoxin, were chemically synthesized and assessed for their disulfide reduction potential, intrinsic folding of disulfides, and disulfide isomerization activity on α-conotoxin ImI. The reduction potential of the disulfide of peptides varies from −189 to −344 mV, which is within the range observed for the redox family of proteins that modulates the folding of protein disulfides. The oxidative folding studies confirm the significance of the tryptophan residue in engaging Li520 in disulfide-exchange reactions and the role of proline hydroxylation in extending the lifetime of Li520 in a reduced free thiol state. Studies of quenching of tryptophan fluorescence by the disulfide in situ folding reaction in conjunction with the optimized structures by density functional theory (DFT) confirm the difference in conformation of disulfides between the native and mutant peptides. Interestingly, the native peptide Li520/Li504 shares a similar disulfide conformation of (−,−)AntiRHHook with the redox family of proteins known to modulate disulfides, particularly in lieu of the tetrapeptide of glutaredoxin, deviating from its disulfide conformation compared to its naive protein. Analysis of the precursor gene sequences of M-superfamily conotoxins revealed the presence of Li520 in different cone snail species with distinct food habits and possible modes of evolution through the diversification of cysteine motifs. The results of the report suggest that the short redox conopeptide Li520 has evolved to facilitate the oxidative folding of conotoxins and may be useful to develop as reagents for the synthesis of therapeutically important cysteine-rich peptides.

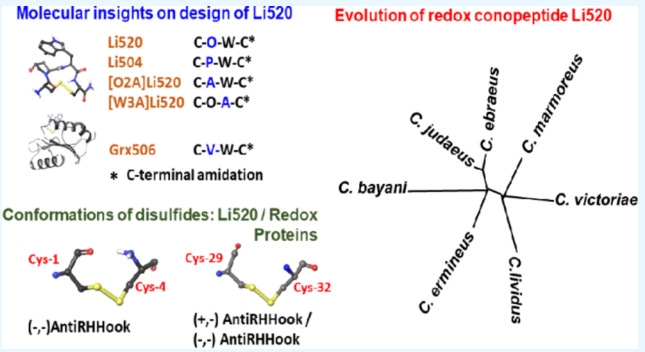

1. INTRODUCTION

Disulfide-rich conotoxins are arsenals that mediate the chemical basis of communication between cone snails and their prey, predators, and competitors in the ecological niche of a diverse marine environment.[1−4] Successful continuation and diversification of lineages of cone snails in the biotic chain is largely dependent on conotoxins and thus imposes evolutionary pressure for their efficient synthesis in the venom duct.[5−8] The expression of hundreds of conotoxins in native form in the venom duct, despite multiple intramolecular disulfide bonds, further supports the evolution of oxidative folding machinery in the cone snail venom duct.[5,9−11] Delineation of the folding machinery of conotoxins resulted in protein disulfide isomerase (PDI),[11−15] cone snail-specific protein disulfide isomerase (csPDI),[12] peptidylprolyl cis−trans isomerase (PPI),[16] prolyl-4-hydroxylase (P4H),[17,18] and immunoglobulin-binding protein (BiP).[19] Recently, a new component of the folding machinery of conotoxins has been characterized as a "redox conopeptide" that catalyzes the formation of native disulfide bonds of conotoxins.[20,21] Such a class of peptides have been characterized by the venom duct transcriptome of *C. lividus*, *C. frigidus*, and *C. amadis* collected from the east coast of India, and they share similar -C-X-X-C- motifs. Unlike the protein component of the folding machinery, these redox peptides are expressed like conotoxins as precursor prepropeptides with mature peptides at the C-terminus and contain posttranslational modifications.[20,21] Conotoxin genes rapidly evolve and contain a conserved signal sequence, moderately variable pro-region, and a hypervariable toxin region with a conserved disulfide framework.[5,6] The evolutionary optimization of conotoxins to have specific activity toward ion channels/receptors in excitable neuronal circuits has been demonstrated and representative examples

Received: February 1, 2024
Revised: July 31, 2024
Accepted: August 13, 2024
Published: August 28, 2024

Table 1. Calculated and Observed Mass of the Synthetic Peptides[a]

		reduced peptide		oxidized peptide	
sr. no.	peptide	[M + H] + cal.	[M + H] + obs.	[M + H] + cal.	[M + H] + obs.
1	[O2A]Li520	481.5 Da	481.1 Da	479.5 Da	479.1 Da
2	[W3A]Li520	408.5 Da	408.1 Da	406.5 Da	406.1 Da
3	Grx506	509.6 Da	509.2 Da	507.6 Da	507.2 Da

[a]Note: Mass spectrometric characterization of Li520, Li504, and α-conotoxin ImI aligns with the previous reports.[20]

are ω-conotoxins targeting Ca(2+) channels,[5,22] α-conotoxins acting on nAChRs,[23] and μ-conotoxins on the Na(+) channel.[24,25] The current report assesses if the snail has employed any such evolutionary optimization on redox conopeptides toward their disulfide isomerization activity with the shortest peptide Li520 as a model example. Concerted efforts toward developing these unexplored redox conopeptides as adjuvants of in vitro oxidative folding of conotoxins are poised to accelerate the large-scale synthesis of therapeutically useful disulfide-rich conotoxins.

The redox conopeptide Li520 (COWC*, *: C-terminal amidation) has unique structural features with an active -C-X-X-C- motif containing a posttranslationally modified proline residue and a bulky least propensic tryptophan residue.[20] The modified 4-trans-hydroxyproline residue regulates the deprotonation of the N-terminal cysteine thiol by shifting the geometry of the Cys-1-Hyp2 peptide bond between cis and trans configuration.[20] The tryptophan residue is involved in proline-aromatic interaction in the folded peptide[20] and such interactions have been identified in the short single disulfide-containing contryphan and Vi805 conopeptides.[26,27] The current report aims to evaluate the significance of noncysteine residues of Li520 on its structure and function, and thereby to shed light on the evolution of Li520 to facilitate the oxidative folding of cysteine-rich conotoxins. The method of alanine scanning mutations of noncysteine residues coupled to structure−function studies has been adopted to unravel the evolutionary optimization of conotoxins.[5,28,29] The current report has also employed the same approach on Li520 to understand its evolutionary optimization by mutating the individual noncysteine residues and replacing the 4-trans-hydroxyproline with the proline residue. The tryptophan-containing glutaredoxin active motif, named Grx506, was also chosen as the control for the studies. The desired peptides were chemically synthesized, structures were deduced by density functional theory (DFT), and functions were evaluated by determining the reduction potential of cysteine disulfide[30,31] and by performing intrinsic/assisted oxidative folding studies. Given previous reports assigning the conformation of cysteine disulfides to the functions of proteins, the current studies also compared the conformation of cysteine disulfides in Li520/its analogues with that of the redox family of proteins, which are known to modulate the disulfides of the polypeptide. The results indicate that both proline and tryptophan residues play an essential role in the structure and functions of Li520 and support its evolutionary optimization to aid the folding of conotoxins.

2. MATERIALS AND METHODS

2.1. Materials. Solid-phase peptide synthesis chemicals and protected amino acids were purchased from Avra Synthesis Pvt. Ltd., India. Reduced glutathione (GSH) and oxidized glutathione (GSSG) were obtained from Merck, India. Deprotection and buffer reagents were purchased from SD Fine Chemicals, India. HPLC grade solvents were obtained from Merck, India. Dimethyl sulfoxide (DMSO) was purchased from Merck, India.

2.2. Peptide Synthesis and Purification. Li520, Li504, [O2A]Li520, [W3A]Li520, Grx506, and α-conotoxin ImI were synthesized manually by the standard solid-phase peptide synthesis method on rink amide resin using Fmoc-chemistry and activation of the C-terminus of protected amino acids by HBTU/DIPEA.[20] The peptides were cleaved off from resin using Reagent-K [TFA/H2O/Phenol/EDTA/Thioanisol (85:5:5:2.5:2.5)] by incubating for a period of 3 h. The cleaved peptides were precipitated and washed 4−5 times using cold, dry ether. The crude peptides were analyzed on an analytical Phenomenex C_{18} column (250 mm × 4.6 mm, 5 μM) over the linear gradient of acetonitrile and detected at 226 nm. The reduced crude peptides were dissolved in 50% acetonitrile containing 5% DMSO and incubated with 100 mM NH_4HCO_3 (pH 8) at room temperature by shaking occasionally for about 16 h. The reactions were quenched by using TFA by acidification. The reduced/oxidized crude peptides were purified in an RP-HPLC semipreparative C_{18} column (250 mm × 10 mm) over a linear gradient of 0.1% TFA acetonitrile at the flow rate of 2.0 mL/min and the elution was monitored at 226 nm. The peptides were quantified using UV spectroscopy, immediately lyophilized, and stored at −20 °C. The reduced and oxidized pure peptides were subjected to mass spectrometry.

2.3. Mass Spectrometry. Mass spectrometric characterization of the synthetic peptides was achieved using an Agilent Q-TOF mass spectrometer (Agilent Technologies India Pvt. Ltd.). Table 1 provides the calculated and observed mass of the synthetic peptides.

2.4. Determination of the Reduction Potential of Cysteine Disulfides. *2.4.1. Thiol−Disulfide-Exchange Reaction Coupled to RP-HPLC.* The reduction potential of Grx506 was calculated using GSH/GSSG and those of [O2A]Li520 and [W3A]Li520 using dithiothreitol (DTT), respectively. Briefly, 1 mM oxidized Grx506 was incubated with 10:1 redox buffer GSH/GSSG in 100 mM NH_4HCO_3 to maintain the pH 8 at room temperature. Similarly, 1 mM oxidized [O2A]Li520/[W3A]Li520 was incubated with 500 μM DTT in 100 mM NH_4HCO_3 at pH 8 and room temperature. The reactions were quenched by acidifying using TFA at regular intervals of time, and the reaction mixtures were separated over the linear gradient of acetonitrile containing 0.1% TFA on an analytical C_{18} column using RP-HPLC and detected at 226 nm. The amounts of oxidized and reduced peptides and GSH, GSSG, or DTT (reduced and oxidized) at equilibrium were estimated by integrating the area under the curve of the elution profile using the protocol provided by Shimadzu Corp. The reduction potential of the cysteine disulfides of the peptides was calculated using the Nernst equation, as described previously.[20,21] The reported

https://doi.org/10.1021/acsomega.4c01028
ACS Omega 2024, 9, 37596−37609

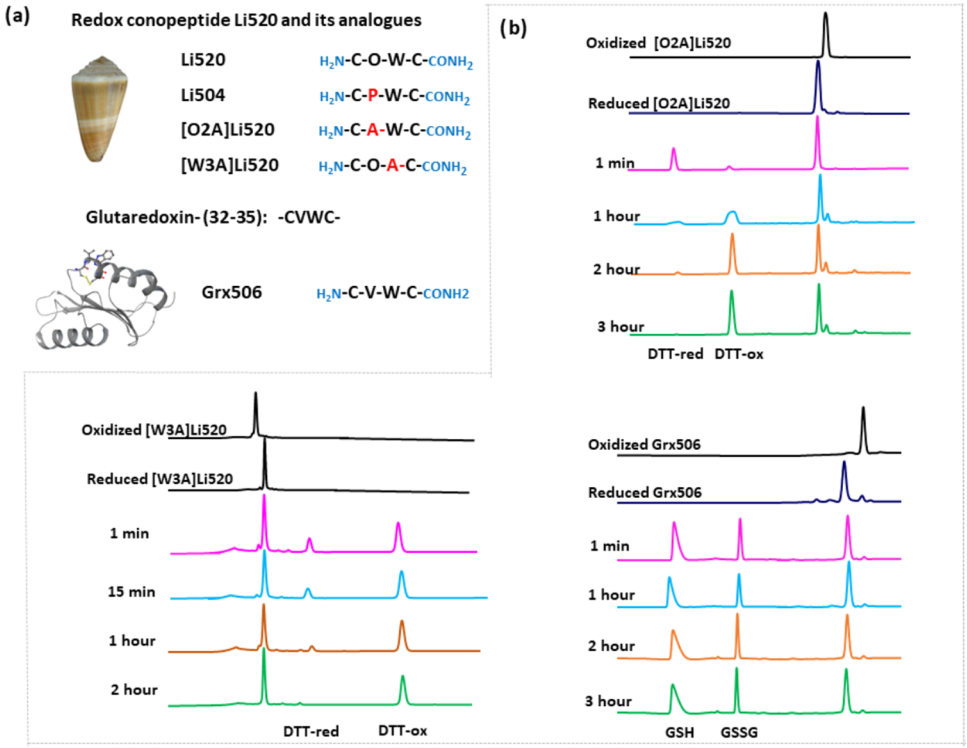

Figure 1. (a) Peptide sequences of Li520 and its analogues, including the glutaredoxin active-site motif. The inset shows the cone shell of *C. lividus*[20] and the crystal structure of glutaredoxin (PDB ID: 3NZN). (b) RP-HPLC elution profiles were drawn at regular intervals during the thiol−disulfide-exchange reaction. [O2A]Li520 and [W3A]Li520 were incubated with DTT and Grx506 with GSH:GSSG redox buffer.

reduction potentials are the average values derived from three independent experiments.

2.4.2. Computational Method. The optimized three-dimensional (3D) structures of reduced and oxidized [O2A]-Li520, [W3A]Li520, and Grx506 were used to calculate the reduction potential of cysteine disulfide on the Jaguar of the Schrodinger Material Science Suite platform. Gibbs free energy (ΔG) change between the oxidized and reduced states of the peptides was calculated using the reaction tool. SCF spin treatment was unrestricted with maximum grid density in the B3LYP-D3 functional combined with a 6-31 G** basis set with polarization function on all atoms. The reduction potential was calculated using $E = \Delta G/nF$, where n is the number of electrons transferred and F is Faraday's constant.

2.5. Optimization of the 3D Structure of Peptides Using DFT. The 3D structures of the peptides were deduced using the density functional theory on Schrodinger Material Science Suite software. The total number of atoms in the peptides varies from 100 to 102. The peptide sequences were constructed using "Build biopolymer" from the sequence tool of Maestro and minimized using the OPLS4 force field in the gaseous state. Subsequently, peptides were subjected to the "Conformational search" tool to identify the low-energy conformer and optimized using the "Optimization" tool on the Jaguar platform. B3LYP-D3 was functional in combination with a 6-31 G** basis set with a polarization function on all atoms chosen with an ultrafine accuracy level. The SCF spin treatment was unrestricted, and the maximum iteration step and grid density were set to 100. The measure tool measured the dihedral angles of optimized 3D structures, and superposition was done by the quick align tool. Ramachandran map was plotted using the Ramachandran Plot tool of Schrodinger software. Interaction toggle was used to identify the hydrogen bond interactions in the optimized structures.

2.6. Oxidative Folding of Li520 and Analogues. *2.6.1. RP-HPLC.* 50 μM reduced peptides were incubated with 5:1 GSH/GSSG in 100 mM NH_4HCO_3 (pH 8) at room temperature. The reactions were quenched at different time intervals using TFA by acidification and separated by RP-HPLC using an analytical Phenomenex C_{18} column (250 mm × 4.6 mm, 5 μM) over the linear gradient acetonitrile containing 0.1% TFA. The flow rate was 1 mL/min and was detected at 226 nm. The amount of oxidized and reduced peptides was estimated by integrating the area under the curve of the elution profile using the protocol provided by Shimadzu Corp. The graphs of variation of reduced/oxidized form as a function of time were plotted using Origin Software. The error bars were calculated from three independent experiments.

2.6.2. Fluorescence Spectroscopy. Fluorescence measurements were performed on a FluoroMax Plus fluorometer (HORIBA Scientific). The samples were excited at wavelength 280 nm, and emission spectra were recorded from 290 to 500 nm. All of the folding experiments were conducted in the fluorescence cuvette of path length 1 cm. 50 μM reduced peptides were incubated with 5:1 GSH/GSSG in 100 mM NH_4HCO_3 (pH 8) at room temperature in the fluorescence cuvette. 3 mL was the total volume of the reaction. Immediately, the reaction was subjected to recording the fluorescence spectra at regular intervals of time. The maximum fluorescence intensity for the peptides was measured at 358 nm. The graphs of fluorescence intensity versus time were plotted using Origin software. The error bars represent the data from three independent experiments.

2.7. Li520 and Its Analogues-Assisted Oxidative Folding of α-Conotoxin Iml. The oxidative folding of α-

https://doi.org/10.1021/acsomega.4c01028
ACS Omega 2024, 9, 37596−37609

Table 2. Reduction Potential and Folding Rate Constant of Li520 and Its Analogues

peptides	reduction potential (mV)		folding rate constant (min^{-1})	
	thiol-disulfide-exchange method	computational method	intrinsic	globular form of α-conotoxin ImI
Li520[a]	−284	−240	0.71	0.05
Li504[a]	−278	−281	1.02	0.04
[O2A]Li520	−260	−189	0.83	0.04
[W3A]Li520	−344	−277	0.63	0.07
Grx506	−337	−200	0.72	0.13

[a]As reported previously.[20]

conotoxin ImI was conducted without and with reduced Li520, [O2A]Li520, [W3A]Li520, and Grx506. Note that the comparison of oxidative folding of α-conotoxin ImI with Li520 and Li504 has been reported previously.[20] 50 μM reduced α-conotoxin ImI and 5 mM reduced Li520 and its analogues were incubated in the redox buffer 1 mM GSH/GSSG (1:1 ratio) in 100 mM NH_4HCO_3 at room temperature. The folding reaction was carried out at pH 8 over a period of 3 h. The reaction was quenched by acidification with TFA at regular intervals of time. The folding reaction mixture was separated by RP-HPLC using an analytical Phenomenex C_{18} column (250 mm × 4.6 mm, 5 μM) over the linear gradient acetonitrile containing 0.1% TFA. The flow rate was 1 mL/min and detected at 226 nm. As described previously, based on the mass and relative elution profile under RP-HPLC, the disulfide foldamers of α-conotoxin ImI were established. The yield of bead, ribbon, and globular fold of α-conotoxin ImI was calculated by integrating the area under the curve using the Shimadzu Corp. protocol. The graph of accumulation of disulfide foldamers of α-conotoxin ImI versus time was plotted using Origin Pro software. The error bars represent data from three independent experiments.

2.8. Conformational Analysis of Cysteine Disulfides in the Redox Family of Proteins. A total of 119 structures of thioredoxin (Trx), 46 of glutaredoxin, 22 of protein disulfide isomerase (PDI), and 57 of thioredoxin reductase (Trr) were retrieved from PDB. Most of them are crystal structures with a resolution cutoff of ≤2.0 Å. The five side-chain torsional angles of cysteine disulfides of redox proteins $\chi_1\ \chi_2\ \chi_3\ \chi_2'\ \chi_1'$ and the disulfide strain energy were determined using the disulfide bond dihedral angle energy server (https://services.mbi.ucla.edu/disulfide/). Conformations of cysteine disulfides were defined using the nomenclature system defined by Govindu et al., based on the sign of five side-chain torsional angles.[32,33] The sign of $\chi_1\ \chi_2\ \chi_3\ \chi_2'\ \chi_1'$ torsional angles for (+,−)-AntiRHHook disulfide conformation is (+,−,+,+,−) and that of the (−,−)AntiRHHook disulfide is (−,−,+,+,−).

2.9. Database. The precursor prepropeptide sequences of conotoxins were retrieved from the ConoServer (https://www.conoserver.org/) database. Some of the sequences were identified through the protein BLAST search tool (https://blast.ncbi.nlm.nih.gov/Blast.cgi). Multiple-sequence alignment was achieved using Clustal omega. The phylogenetic tree was constructed using Phylip. The list of M-superfamily conotoxins was retrieved from Conoserver. The 3D structures of proteins were processed using the Glide platform of Schrodinger software. The statistical analysis was carried out using GraphPad software (https://www.graphpad.com/quickcalcs/ttest1.cfm).

3. RESULTS

3.1. Reduction Potential of [O2A]Li520, [W3A]Li520, and Grx505. The redox conopeptide Li520 is a short tetrapeptide derived from *C. lividus* and contains hydroxyproline and tryptophan residues within the disulfide loop. The noncysteine residues of Li520 have been systematically replaced with alanine to yield analogues, namely, [O2A]Li520 and [W3A]Li520 (Figure 1a). A search of PDB for the -CXWC- motif resulted in glutaredoxin (PDB: 3NZN) with an active-site motif -CVWC-.[34] The tetrapeptide motif of glutaredoxin was labeled as Grx506 (Figure 1a). The desired peptides were chemically synthesized by a solid-phase peptide synthesis methodology (Scheme S1) and characterized using RP-HPLC and mass spectrometry. Figures S1−S6 provide the RP-HPLC elution profile, ESI-MS, and ESI-MS/MS of the synthetic peptides' reduced free thiol and oxidized disulfide forms. The shift in retention times of the elusion profile and reduction in the mass by two Dalton atoms confirm the presence of disulfide bonds in the oxidized synthetic peptides. The peptides [O2A]Li520, [W3A]Li520, and Grx506 were subjected to the calculation of reduction potentials using both thiol−disulfide-exchange reactions and the computational method. In the case of [O2A]Li520, the reduced and oxidized peptides at equilibrium were detected in the glutathione redox buffer, whereas in the case of Grx506, the reduced and oxidized states of the peptides were detected with DTT. Figure 1b shows the elution profiles of the redox conopeptide upon equilibration with redox buffers. The estimated reduction potential for [O2A]Li520 is −260 mV, [W3A]Li520 is −344 mV, and Grx506 is −337 mV. As described previously, computational methods can also calculate the reduction potentials from the optimized structures of the reduced and oxidized states of the peptides. The desired peptides were optimized using Schrodinger Material Science Suite platforms; the ΔG was calculated for the reduction of the corresponding peptide disulfide (Figure S7), and the reduction potential was calculated as described in the Materials and Methods section. Table 2 provides the reduction potentials for peptides [O2A]Li520, [W3A]Li520, and Grx506. As reported previously, the estimated reduction potential of Li504 and Li520 using glutathione/DTT buffer is −281 and −240 mV, and that of the computational method is −278 and −284 mV, respectively.[20] The reduction potential of cysteine disulfide for Li520 and the analogues, including Grx506, is within the range observed for the redox proteins that catalyze the oxidative folding of disulfide-rich polypeptides. These peptides were further subjected to folding studies: (i) intrinsic folding/self-folding in GSH/GSSG redox buffer and (ii) redox-peptide-assisted folding of α-conotoxin ImI in GSH/GSSG redox buffer.

https://doi.org/10.1021/acsomega.4c01028
ACS Omega 2024, 9, 37596−37609

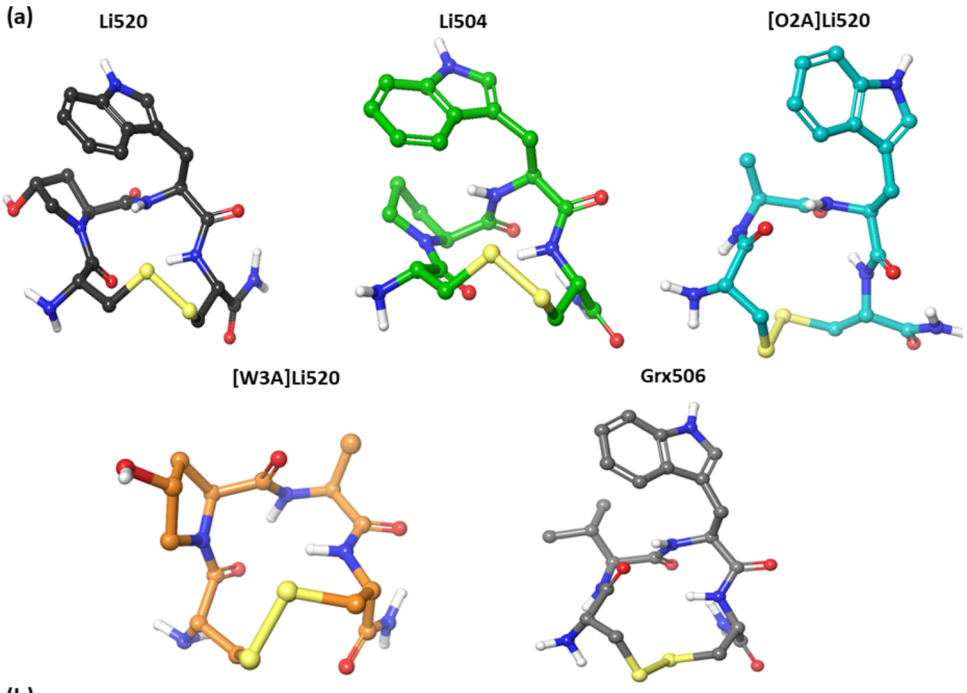

(b)

Peptides	Torsional angles of cysteine disulfide					Sign	Disulfide conformations	DSE (kJ/mol)
	(X1)	(X2)	(X3)	(X2')	(X1')			
Li520	-171.5	-141.6	77.6	75.1	-70.4	−,−,+,+,−	(-,-)AntiRHHook	11.5
Li504	-171.4	-141.5	77.2	74.9	-68.1	−,−,+,+,−	(-,-)AntiRHHook	11.7
[O2A]Li520	18.63	65.3	108.4	-70.1	-59.6	+,+,+,−,−	(+,-)SynRHHook	21.3
[W3A]Li520	-153.8	-76.0	-91.1	97.2	31.4	−,−,−,+,+	(-,+)SynLHHook	24.2
Grx506	30.3	61	97.2	-150.8	62.1	+,+,+,−,+	(+,+)SynRHHook	16.1

Figure 2. (a) Optimized 3D structures of [O2A]Li520, [W3A]Li520, and Grx506 deduced by DFT in the gas phase. The previously reported 3D structure Li520 deduced by DFT is also included for reference. Note that the 3D structures of Li520 and Li504 are similar. (b) Conformation of cysteine disulfide in the optimized structures of Li520 and its analogues. Side-chain torsional angles and disulfide strain energy are also indicated.

3.2. Conformations of Cysteine Disulfides in Li520 and Its Analogues. The 3D structures of [O2A]Li520, [W3A]Li520, and Grx506 were optimized using the density functional theory (DFT) as described previously.[20] Note that the 3D structures of Li520 and Li504 deduced using DFT were reported previously.[20] Figure 2a shows the optimized 3D structures of Li520 and its analogues, including Grx506, using DFT in the gaseous phase. Ramachandran angles of the optimized peptides are well within the allowed region (Figure S8). Figure S9 shows the hydrogen bonding pattern in Li520 and its analogues. The β turn conformation with Cys-4-NH to Cys-1-CO has been observed in Li520. However, such hydrogen bond networks were not observed in [O2A]Li520 and [W3A]Li520. In [O2A]Li520 the hydrogen bond network was observed from Trp-3-NH to Cys-1-CO and from Cys-4-NH to Ala-2-CO. Similarly, in [W3A]Li520, the hydrogen bond was observed between Ala-3-NH and Cys-1-CO. The C-terminal amide protons are engaged in hydrogen bonding with the Ala-3 carbonyl group. In the case of Grx506, the hydrogen bonding network was observed from Trp-3-NH to Cys-1-CO and from amide protons to the Val-2-CO group. The main structural difference observed between Li520 and Li504 is the ring puckering between 4-trans-hydroxyproline and proline residues.[20] The optimized structures indicate the structural differences in Li520 and its analogues. Figure 2b provides the conformations of cysteine disulfides and disulfide strain energy in the optimized 3D structures of Li520 and its analogues. The conformation of cysteine disulfides of Li520 and Li504 is (−,−)AntiRHHook. The disulfide strain energies are also similar between Li520 and Li504. In the analogue, [O2A]-Li520 and [W3A]Li520 is (+,−)SynRHHook and (−,+)SynLHHook, respectively. Further, the disulfide strain energy in the analogues of Li520 is increased by 2-fold. In the case of Grx506, the disulfide conformation is (+,+)SynRHHook. In contrast, the conformation of disulfide in glutaredoxin is (+,−)AntiRHHook. The disulfide strain energies for cysteine disulfide in Grx506 and glutaredoxin are in the same range. The above studies indicate that the mutation of non-Cys residues in Li520/Li504 leads to distortion in the conformation of cysteine disulfides.

3.3. Intrinsic Folding Studies of Li520 and Its Analogues. The intrinsic or self-folding of Li520 and its analogues in glutathione redox buffers was probed using RP-HPLC and fluorescence spectroscopy.

3.3.1. RP-HPLC. Figure 3a shows the RP-HPLC elution profiles of oxidative folding of Li520 and its analogues in glutathione buffer as a function of time. Note that the detectable changes in early folding events between the peptides

https://doi.org/10.1021/acsomega.4c01028
ACS Omega 2024, 9, 37596−37609

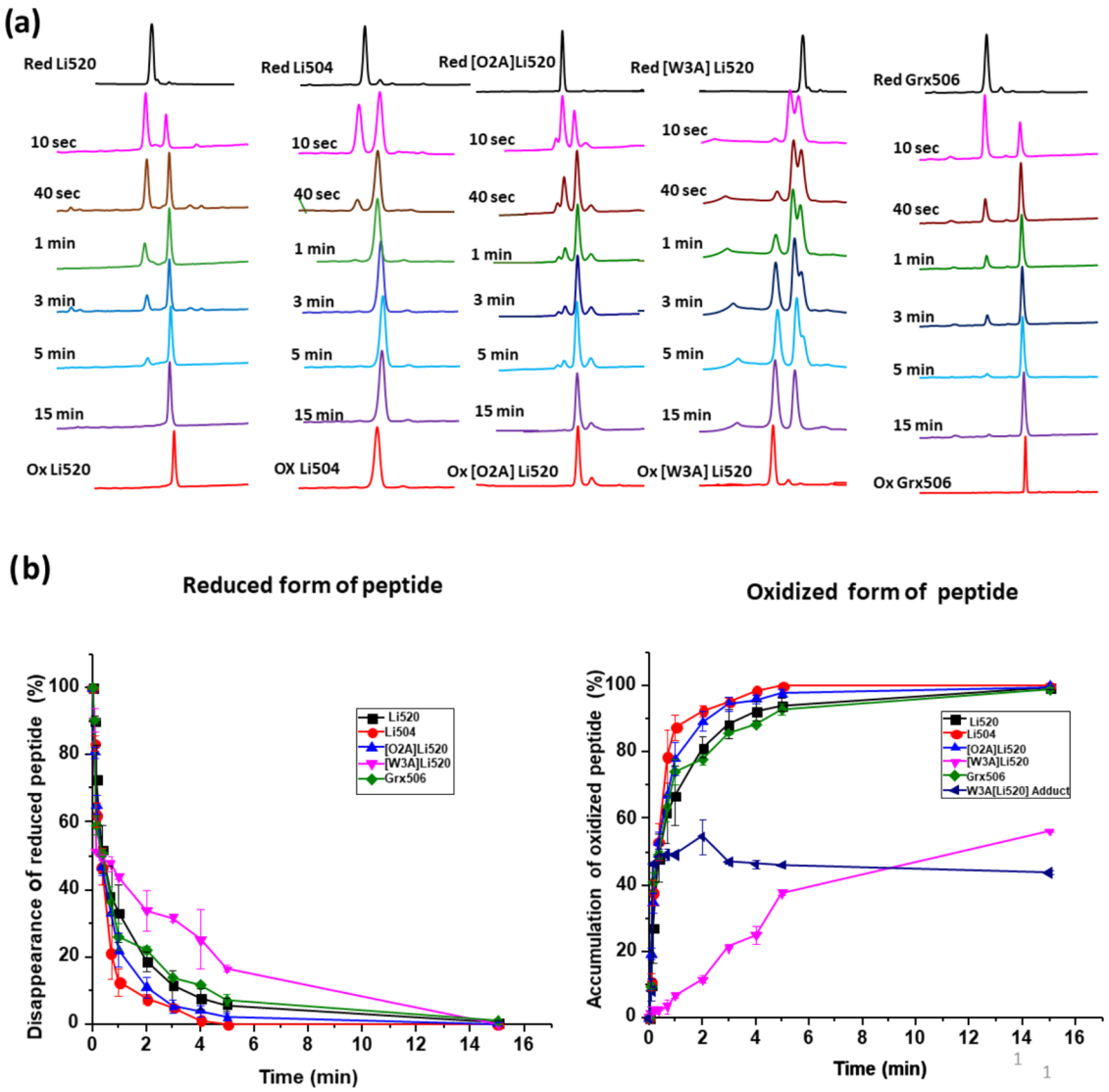

Figure 3. Intrinsic folding of Li520 and its analogues monitored using RP-HPLC. (a) Elusion profiles are drawn at regular intervals of time. The reduced free thiol and oxidized disulfide forms are also included. (b) Disappearance of the reduced form and accumulation of the oxidized form as a function of time. The profile of [W3A]Li520 adduct with glutathione is also indicated in the graph of the oxidized form.

were observed at a 5:1 ratio of GSH and GSSG. The distinct folding events were mainly observed for peptides Li504 and [W3A]Li520 (Figure 3a), which is apparent from the comparison of the intrinsic folding of Li520 and Li504. The proline hydroxylation may retard the formation of a disulfide bond. A notable amount of Li520 exists in the reduced free thiol form even in the late folding events compared to Li504. Thus, the posttranslational modification of 4-trans-hydroxylation of proline in Li520 may be important in extending the free thiol state during the folding reaction. These observations are consistent with previous reports of the hydroxyl group of hydroxyproline interacting with the Cys-1 thiol of Li520.[20] The difference between the disappearance of the reduced form and accumulation of the disulfide form is statistically insignificant among peptides Li520, [O2A]Li520, and Grx506 in the early folding events (Figure 3b). However, a significant difference is observed between [O2A]Li520 and Grx506 in the late folding events. The paired *t* test two-tailed *P*-value between [O2A]-Li520 and Grx506 at 2 min for the disappearance of the reduced form is 0.0394, and that of the accumulation of oxidized form is 0.0478. In the case of [W3A]Li520, a significant amount of adduct accumulates during the folding events, which retards the formation of the disulfide form (Figure 3a,3b). Figure S10 shows the ES-MS and ESI-MS/MS spectra of the adduct observed in the folding events of [W3A]Li520. The observed mass of the adduct of [W3A]-Li520 is 713 Da, which could be ascribed to the single glutathione adduct of the peptide. A facile formation of a_1 ion was observed at m/z 381 during ESI-MS and ESI-MS/MS (Figure S10). These fragment ions correspond to the N-terminus Cys-1 of [W3A]Li520 bearing glutathione through mixed disulfide. The reason for such a facile cleavage of the adduct to form an a_1 ion during MS and MS/MS requires further investigations. The observed fragment ions for m/z 381 are consistent with the sequence of glutathione. These mass spectrometric studies confirm the formation of a glutathione adduct in the folding of [W3A]Li520. It is evident from Figure 3b that the accumulation of adduct retards the formation of the oxidized form, indicating the importance of the participation of the tryptophan residue in Li520 in the thiol−disulfide-exchange reaction. Table 2 provides the rate constants for the intrinsic folding of Li520 and its analogues. The least

https://doi.org/10.1021/acsomega.4c01028
ACS Omega 2024, 9, 37596−37609

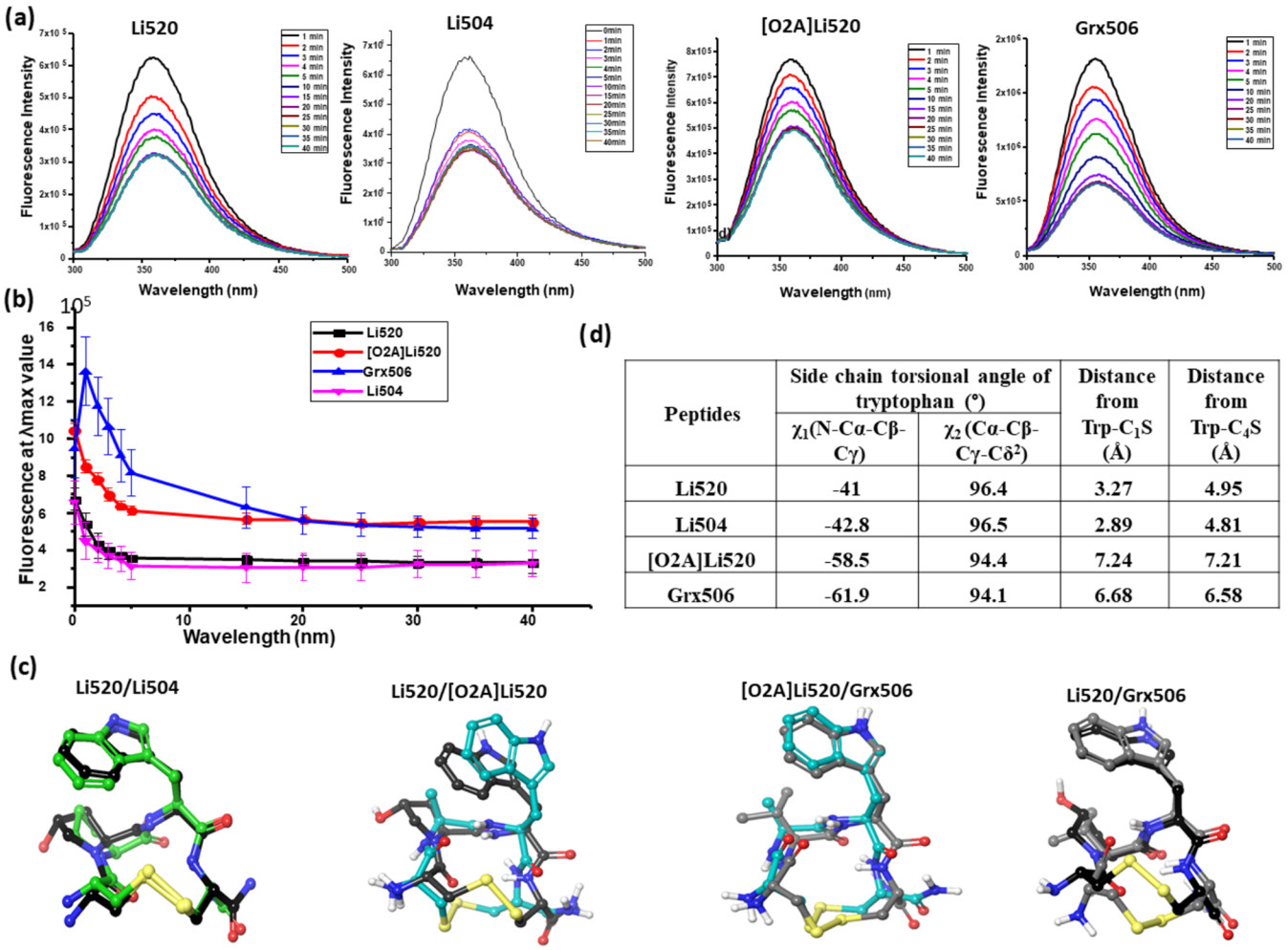

(d)

Peptides	Side chain torsional angle of tryptophan (°)		Distance from Trp-C_1S (Å)	Distance from Trp-C_4S (Å)
	χ_1(N-Cα-Cβ-Cγ)	χ_2 (Cα-Cβ-Cγ-Cδ²)		
Li520	-41	96.4	3.27	4.95
Li504	-42.8	96.5	2.89	4.81
[O2A]Li520	-58.5	94.4	7.24	7.21
Grx506	-61.9	94.1	6.68	6.58

Figure 4. Intrinsic folding of Li520 and its analogues monitored using fluorescence spectroscopy. (a) Fluorescence spectra recorded at regular intervals of time during the folding reaction for the corresponding peptide. (b) Fluorescence intensity at λ_{max} as a function of time. (c) Superposition of a pair of the optimized 3D structures of peptides highlighting the orientation of tryptophan and cysteine disulfide. (d) Summary of side-chain torsional angles of tryptophan and distance between tryptophan and the disulfides in the optimized structures of the peptides.

propensic and bulky tryptophan residue bears a special significance toward the design of Li520 by *C. lividus* to modulate the disulfide formation.

3.3.2. Fluorescence Spectroscopy. It has been reported that the disulfides act as a quencher of tryptophan fluorescence in various redox family proteins.[35−38] Thus, this study has monitored the fluorescence of tryptophan in Li520, Li504, [O2A]Li520, and Grx520 during folding as a function of time using a fluorescence spectrometer. The intrinsic/self-folding conditions are similar for both HPLC and fluorescence methods. The fluorescence spectra of the peptides during folding were recorded as described in the Materials and Methods section. Figure 4a shows the fluorescence spectra of Li520, Li504, [O2A]Li520, and Grx506 as a function of time during oxidative folding in glutathione redox buffer. Figure S11 shows the fluorescence spectra of Li520, Li504, [O2A]Li520, and Grx506 as a function of time in the absence of glutathione redox buffer. The λ_{max} emission wavelength for Li520, Li504, [O2A]Li520, and Grx506 is 358 nm. It is evident from Figures 4a and S11 that the intensity of tryptophan fluorescence decreases with an increase in the time of the folding reaction and subsequently reaches equilibrium. Distinct differences are observed between Li520 and Li504, with the latter reaching the equilibrium at early time points. Li520 and [O2A]Li520 reach the equilibrium at ∼15 min and Grx506 at ∼25 min. These results corroborate the folding studies probed using RP-HPLC (Figure 3a), where the oxidized disulfide form accumulates significantly at 15 min and, in the case of Grx506, some amount of reduced form still exists at that period. The intensity of the tryptophan fluorescence of the peptides is high in the reduced form (Figure S11) and low in the folded disulfide form (Figure 4a), indicating the quenching of tryptophan fluorescence by the disulfides. Figure 4b shows the variation in fluorescence intensity at the emission λ_{max} value as a function of time for Li520 and its analogues. Tryptophan fluorescence intensity differs among the peptides in the reduced free thiol forms by up to ∼60% (Figure S11). In contrast, the area under the curve in RP-HPLC for the reduced free thiol form of the peptides subjected to fluorescence studies varies by only 6%. These observations indicate the difference in the tryptophan environment in the reduced free thiol forms of Li520 and its analogues. The following observations can be derived from Figure 4b pertaining to the fluorescence of tryptophan: (i) the intensity is low in both reduced and oxidized forms of the native peptide Li520, (ii) the intensity increases at an initial point upon addition of glutathione in Grx506, (iii) intensities are similar for disulfide forms of Li520 and Li504 at equilibrium, (iv) intensities are also similar for

https://doi.org/10.1021/acsomega.4c01028
ACS Omega 2024, 9, 37596−37609

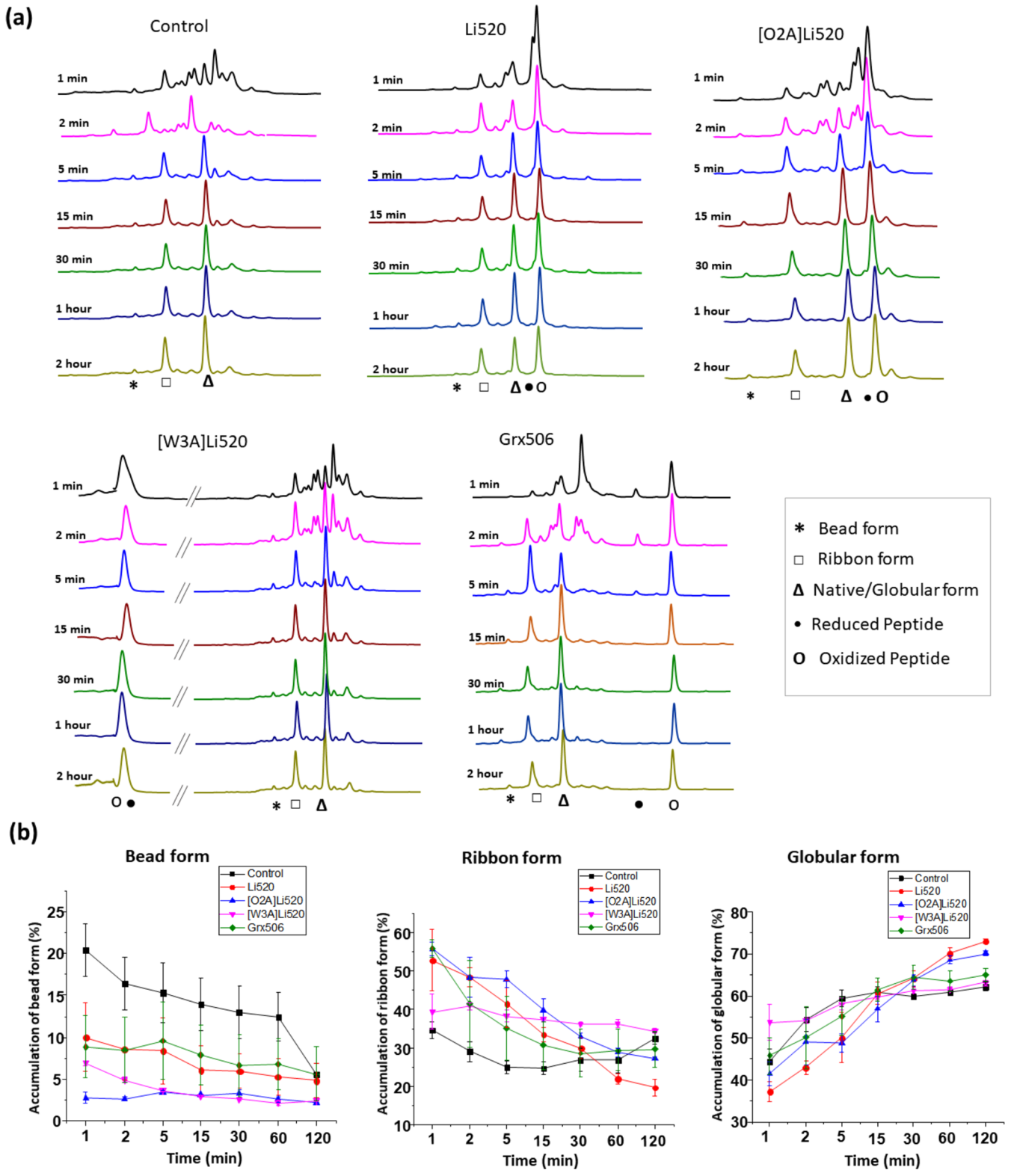

Figure 5. Li520 and its analogues-assisted oxidative folding of α-conotoxin ImI. (a) RP-HPLC elution profiles without and with peptides drawn at regular intervals. The distinct forms of the peptides are indicated. (b) Accumulation of different disulfide foldamers of α-conotoxin ImI as a function of time.

disulfide forms of [O2A]Li520 and Grx506 at equilibrium, and (v) the extent of quenching by disulfide is greater in [O2A]Li520. The report further attempted to correlate the observed differences in the fluorescence of tryptophan to the orientation of tryptophan and disulfide in the optimized 3D structures of the peptides. Figure 4c shows the superposition of the optimized 3D structures of Li520 and its analogues. Figure S12 shows the measurement of the distance between the tryptophan proton and the sulfur of the cysteine disulfide. Figure 4d summarizes the rotamers of tryptophan and the

https://doi.org/10.1021/acsomega.4c01028
ACS Omega 2024, 9, 37596−37609

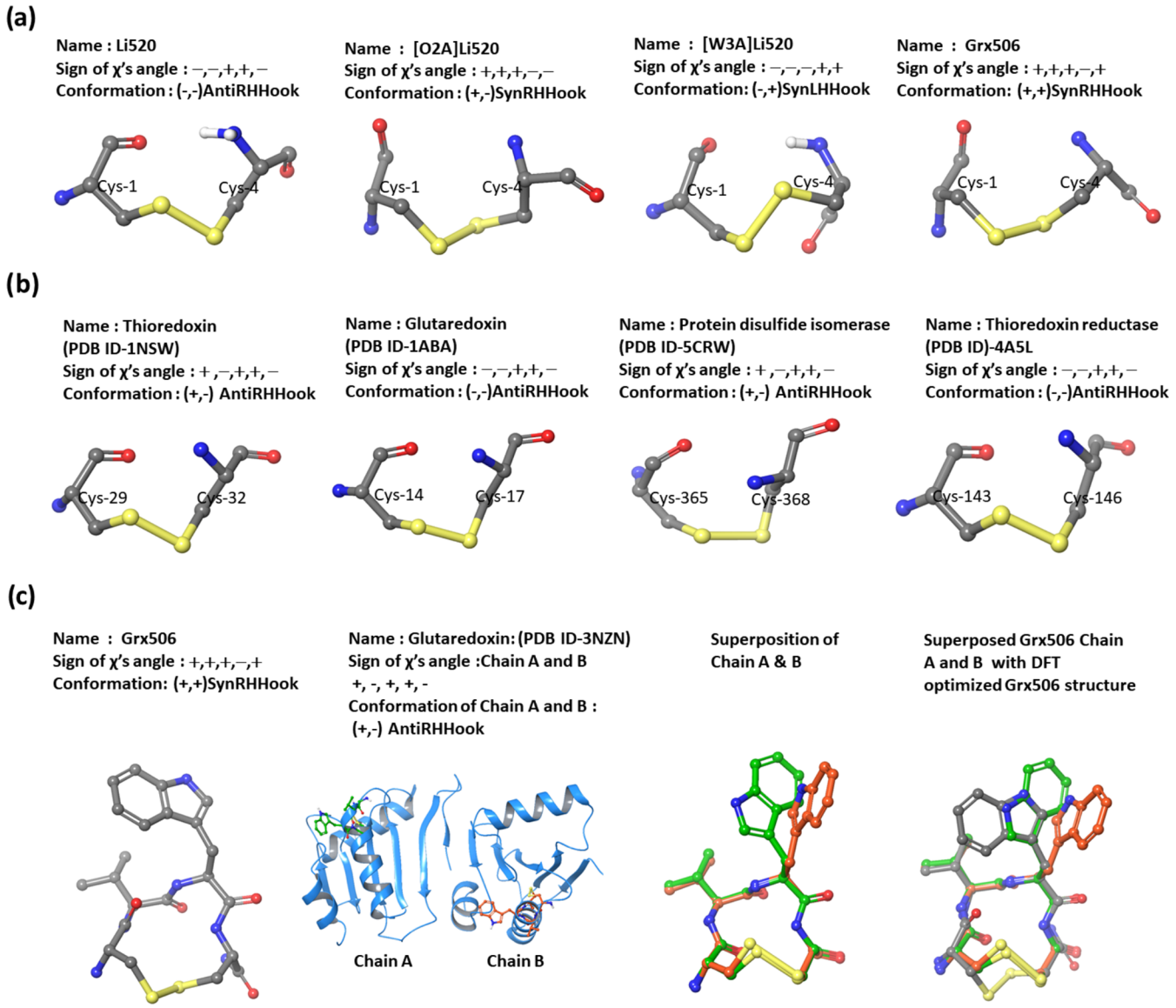

Figure 6. Conformation of cysteine disulfides. (a) Glutaredoxin (Grx), thioredoxin (Trx), protein disulfide isomerase (PDI), and thioredoxin reductase (Trr). (b) Li520 and its analogues. (c) -CVWC- motif in glutaredoxin and Grx506. The PDB ID, sign of torsional angles, and conformation of disulfides are indicated. The superposed structures of the -CVWC- motif are also indicated.

distance between tryptophan and disulfide in the optimized structure of the peptides. The conformation of tryptophan and cysteine disulfide is similar in Li520 and Li504 and is consistent with the observed fluorescence data of the disulfide forms of the peptides. It is evident from Figure 4c that Li520 and [O2A]Li520 have distinct differences in both the orientations of tryptophan and the conformation of cysteine disulfide, and [O2A]Li520 and Grx506 have similar orientations of tryptophan and disulfide, whereas Li520 and Grx506 have similar orientations of tryptophan but differences in cysteine disulfide. It is evident from the crystal structure of glutaredoxin (PDB ID: 3N3Z) that the orientation of the tryptophan residue within the disulfide loop is subtle, and there is a difference between the chains. Dolle et al. reported that tryptophan orientation is relatively rigid in both reduced and oxidized forms of Li520 due to the proline-aromatic CH---π interactions.[20] As the fluorescence quenching is a distance-dependent phenomenon, Figure 4d corroborates the observed difference in quenching of tryptophan fluorescence by the disulfides between Li520 and its analogues. The observed results indicate the proximity of the tryptophan residue to the disulfide, confirming the significance of the tryptophan residue in Li520.

3.4. Li520 and Its Analogues-Assisted Oxidative Folding of α-Conotoxin ImI. This study assessed the influence of Li520 and its analogues on the oxidative folding of α-conotoxin ImI in the glutathione redox buffer. In the previous report, the disulfide isomerase activity of Li520 was demonstrated on α-conotoxin ImI.[20] The study also demonstrates the higher catalytical activity of Li520 compared to Li504 on folding of α-conotoxin ImI.[20] The significance of proline hydroxylation in the disulfide isomerase activity of Li520 was also dealt with in detail in the previous report.[20] The peptide Li520 facilitates the formation of a natively folded globular form of the α-conotoxin ImI. Figure 5a shows the RP-HPLC elution profile of the folding mixture of α-conotoxin ImI as a function of time without and with Li520 and its analogues. The elution profiles at an early point of oxidative

https://doi.org/10.1021/acsomega.4c01028
ACS Omega 2024, 9, 37596−37609

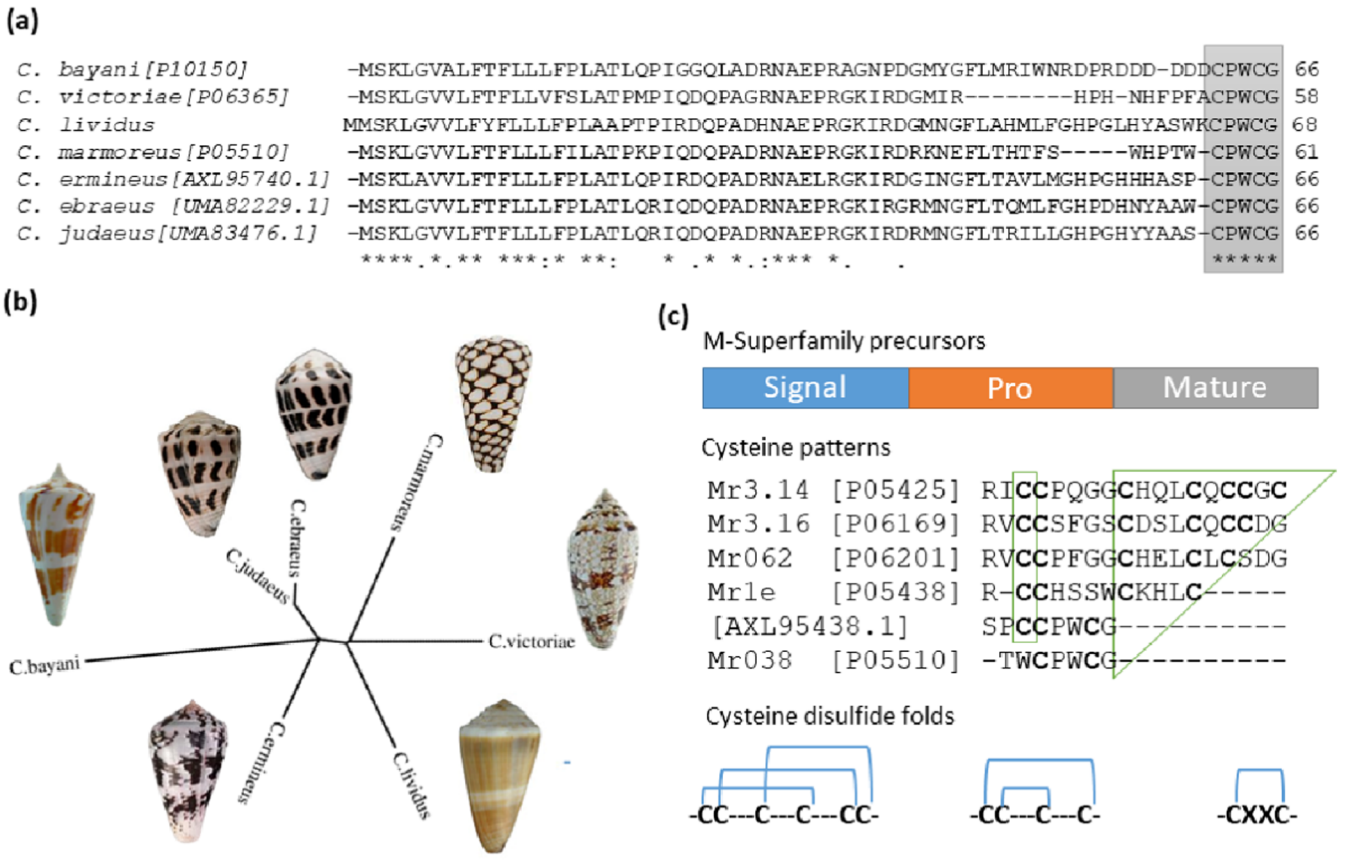

Figure 7. (a) Multiple-sequence alignment of the precursor sequences with the C-terminus Li520 peptide motif derived from different cone snail species. The accession number is indicated, and the required sequence is highlighted. (b) A phylogenetic tree was constructed using the given precursor sequences. The corresponding cone snail pictures are indicated. The citation of cone snail pictures: *C. marmoreus*,[45] *C. victoriae*,[2] *C. ermineus*,[2] *C. bayani*,[2] *C. ebraeus*, *C. judaeus*,[46] and *C. lividus*.[20] (c) Possible mode of the evolution of cysteine motifs of Li520 in M-superfamily conotoxins. All of the sequences are from the same snail, *C. marmoreus*, except [AXL95438.1]. Intramolecular disulfide folds are indicated.

folding distinctly differ between Li520 and its analogues. Figure 5b shows the accumulation of bead, ribbon, and globular forms of α-conotoxin ImI as a function of time in the presence of Li520 and its analogues. It is evident from Figure 5b that the accumulation of the bead form is greatly minimized in the presence of [O2A]Li520 compared with other peptides. However, at equilibrium, accumulation of the bead form is similar between Li520 and [O2A]Li520. The amount of bead form accumulation between Li520 and [O2A]Li520 is insignificant (Table S1). A significant amount of ribbon form accumulates in the presence of Li520, [O2A]Li520, and Grx506 at the initial time point. As the reaction proceeds, the ribbon form decreases to a minimal value from 53 to 19% in the presence of Li520 (Figure 5b). In contrast, in an unaided control reaction, the accumulation of ribbon forms is nearly the same (35−33%) between the initial time point and equilibrium. As is evident from Figure 5b, the accumulation of the natively folded globular form is more in the presence of Li520 than any other analogue, indicating the importance of the naturally designed redox conopeptide Li520 in assisting the oxidative folding of α-conotoxin ImI. The mutant peptide [O2A]Li520 shows similar assisted folding features compared to Li520. However, according to the statistical analysis (Table S1), the native peptide has superior catalytical activity. It is worth mentioning that at equilibrium, [W3A]Li520 does not impact the formation of the native fold, further emphasizing the importance of tryptophan in Li520. Table 2 provides the rate constant for folding the globular form of α-conotoxin ImI with Li520 and its analogues. The monumental work by Safavi-Hemami et al.[19] reported the occurrence of both ribbon and globular forms of α-conotoxin ImI in the venom of *C. imperialis*. They also established the role of a multienzyme complex of PDI, PPI, and BIP, contributing to the folding of the ribbon form of α-conotoxin ImI. Innumerable reports have documented the globular form as the native fold of α-conotoxins. In the above context, Li520 rearranging ribbon to the globular fold of conotoxin ImI bears special significance, further highlighting its importance in the folding of conotoxins.

3.5. Conformation of Disulfides in the Redox Family Protein with CXXC Motif. This study further intended to compare the conformations of disulfides between Li520 and redox family proteins that catalyze the formation of protein disulfides. The previous reports have classified the protein disulfides as structural, allosteric, and catalytic disulfides based on the conformation of cysteine disulfide.[39−41] They have assigned the conformation of +/− RHHook to the catalytic disulfides that regulate oxidation, reduction, and rearrangement of protein disulfides. Thus, the report intended to verify whether the redox conopeptide Li520 shares a conformation similar to the catalytic disulfides of proteins that regulate the disulfide bond formation. The redox family of proteins with -CXXC- motifs can be broadly classified into four distinct classes, namely, glutaredoxin (Grx), thioredoxin (Trx), protein disulfide isomerase (PDI), and thioredoxin reductase

https://doi.org/10.1021/acsomega.4c01028
ACS Omega 2024, 9, 37596−37609

(Trr).[30,42−44] The 3D structures of redox proteins were retrieved from the PDB, and conformations of disulfides were analyzed as described in the Materials and Methods section. Table S2 provides the conformation of disulfides in four distinct classes of the redox family of proteins retrieved from the PDB. Table S3 provides the conformational analysis of cysteine disulfides in glutaredoxin (Grx), thioredoxin (Trx), protein disulfide isomerase (PDI), and thioredoxin reductase (Trr). Schmidt et al. have reported the thioredoxin proteins that possess catalytic disulfides to have +/− RHHook conformations. In this nomenclature of disulfides, the forward and reverse conformations of disulfides are equated like the case of +/− RHHook conformations.[39,40] Govindu et al. have differentiated this confirmation into separate classes; for example, +/− RHHook is differentiated as (+,−)AntiRHHook and (−,+)SynRHHook.[32,33] The report followed the new nomenclature system in the conformational analysis of redox proteins (Tables S2 and S3). It stems from the current analysis that the conformations (−,−)AntiRHHook and (+,−)-AntiRHHook have similar disulfides (Figure S13). The χ_1 angle values of these two conformations are around ±180°. The slight changes in these values confer different names for similar disulfides. Such limitations are previously discussed in the conformational analysis of vicinal cysteine disulfides. Hence, (−,−)AntiRHHook and (+,−)AntiRHHook were treated as the same in the current analysis of redox family protein disulfides (Figure S13). It is evident from Table S3 that nearly 89% of thioredoxin, 92% of glutaredoxin, 57% of protein disulfide isomerase, and 98% of thioredoxin reductase cysteine disulfides have (−,−)AntiRHHook or (+,−)AntiRHHook conformation. Note that the protein disulfide isomerase has a limited number of entries (Table S3). Figure 6a shows the conformation of disulfides in redox family proteins. Figure 6b shows the conformation of disulfides in Li520 and its analogues. The native redox peptide Li520 and the redox family of proteins share the same disulfide conformations of (−,−)AntiRHHook. In contrast, mutant Li520 analogues display different conformations of disulfides. The report further intended to compare the conformations of disulfides of CVWC in the protein glutaredoxin and that of the optimized structure of Gr506 peptide (Figure 6c). In glutaredox (PDB ID: 3NZN), the CVWC motifs in chain-A and chain-B have the same confirmation of (+,−)AntiRHHook (Figure 6c). Interestingly, in the short tetrapeptide Grx506, the CVWC motif has a different conformation of (+,+)-SynRHHook (Figure 6c). These observations indicate that the protein environment is enduring support to the disulfides to have the (+,−)AntiRHHook conformation. The retention of the conformation of catalytic disulfide (−,−)AntiRHHook in the short conopeptide Li520, which was observed in protein disulfide isomerases in lieu of deviation in its analogues, further supports its evolution to catalyze the folding of conotoxins.

4. DISCUSSION

The short peptide Li520 is a novel redox conopeptide belonging to the M-superfamily conotoxins and derived from the venom duct transcriptome of the Indian marine snail *C. lividus* collected from the east coast.[20] A search of databases with the precursor sequence of Li520 resulted in similar polypeptide sequences of the M-superfamily from diverse cone snail species (Figure 7a). Dutertre et al. have reported the novel Mr038 precursor sequence that shares the -CPWC- motif from *C. marmoreus* by the deep venomics and indicated that reliable data was not obtained in MS/MS.[47] Robinson et al. have reported the precursor M_Vc3 that is similar to Mr038 from *C. victoriae* and ascribed it to the constitution of a new class of single disulfide-containing conotoxins.[48] Abalde et al. have reported the precursor of the redox conopeptide under the superfamily M-WF derived from the transcriptome of the venom duct of Chelyconus *C. ermineus* collected from the Atlantic/Indo-Pacific region.[49] Rajaian Pushpabai et al. have reported on the precursor sequence with C-terminus CPWCG peptides deduced by transcriptomic analysis of the venom duct of *C. bayani* collected from the northwest coast of India.[50] Pardos-Blas et al. have reported the comparative venom duct transcriptomic analysis of a special class of *Virroconus* species *C. ebraeus* and *C. judaeus* having precursor sequences of redox conopeptides.[46] Figure 7b provides the phylogeny of cone snails having the Li520 redox conopeptide motif deduced using its precursor M-superfamily sequences. Interestingly, Li520 redox conopeptide motif is detected in the venom duct of piscivores (*C. ermineus*), molluscivores (*C. marmoreus/C. victoriae*), vermivores (*C. lividus/C. bayani*), and also in *Virroconus* (*C. ebraeus/C. judaeus*) species. The occurrence of the Li520 sequence motif in cone snails of different food habits supports the evolution of these peptide motifs rather than accidental occurrence in the venom duct. Unlike conotoxins predominately secreting in the venom,[5,6] the redox conopeptides may work synergistically with the oxidative folding machinery embedded in the membrane of the snail venom duct, obscuring their detection by conventional methods. The increasing efforts of venom duct transcriptomics may further expose the presence of redox conopeptides in diverse cone snail species, and available data strongly point to their evolution in the venom duct.

The report further scrutinized M-superfamily conotoxins and their precursors for the number of cysteine residues in the mature sequence (Table S4). Interestingly, the M-superfamily comprises peptides with varying numbers of cysteine residues from 1 to 8, including the cysteine-free peptide conomorphin.[5,45,51,52] These features indicate the diversification of M-superfamily conopeptides on the evolutionary time scale leading to the genesis of redox conopeptides. Further inspection of M-superfamily peptides derived from *C. marmoreus* revealed the cysteine residues' pruning in the mature peptides (Figures S13 and 7c). Note that the precursor of *C. ermineus* provided the missing link of three cysteine residues at the mature peptide. Conservation of the signal sequence, moderate conservation of the pro-region, and the hypervariable mutation of mature peptide, including cysteine residues and disulfide folds, indicate the possible evolution of redox conopeptides (Figure S13). The molecular-level insights into the folding of Li520 and its analogue and their influence on the oxidative folding of α-conotoxin ImI support that Li520 facilitates the folding of conotoxins. Conformations of cysteine disulfides of redox family proteins predominantly contain (+,−)AntiRHHook/(−,−)AntiRHHook. Figure S14 shows the conformations of cysteine disulfides in a redox protein family. Such unique conformations of cysteine disulfides have been previously reported in redox proteins, indicated as +/− RHHook, which translates to (+,−)AntiRHHook and (−,+)SynRHHook as per the new nomenclature system. Cysteine disulfides in the optimized 3D structure of Li520 have (−,−)AntiRHHook conformation, and that of analogues exhibits deviations in the conformations of disulfide. The retention of the bonafide conformation of cysteine disulfide

https://doi.org/10.1021/acsomega.4c01028
ACS Omega 2024, 9, 37596−37609

that is involved in oxidation, reduction, and rearrangement of disulfide in the short peptide Li520 supports its evolution for facilitating the oxidative folding of conotoxins. The occurrence of a -CPWC- motif in cone snails of three distinct food habits, the enhanced catalytical activity of native peptides, and the retentions of conformations of disulfide of the folding catalyst of proteins support the evolution of Li520 in the venom duct. Increasing attempts at next-generation sequencing of venom duct transcriptome[53−56] may unravel the diversity of redox conopeptides, and the development of reagents based on evolutionarily optimized redox conopeptides may accelerate the in vitro synthesis of conotoxins of therapeutic values.

■ ASSOCIATED CONTENT

Supporting Information

The Supporting Information is available free of charge at https://pubs.acs.org/doi/10.1021/acsomega.4c01028.

Schemes, mass spectra, DFT structures, fluorescence spectra, and conformational analysis of disulfides (PDF)

M-superfamily conotoxins with any Cys framework retrieved from ConoServer database (XLSX)

■ AUTHOR INFORMATION

Corresponding Author

Konkallu Hanumae Gowd − *Department of Chemistry, School of Chemical Sciences, Central University of Karnataka, Kalaburagi 585367 Karnataka, India;* orcid.org/0000-0002-8991-9368; Phone: 08477-226748; Email: khgowd@cuk.ac.in; Fax: 08477-226703

Authors

Shweta Dhannura − *Department of Chemistry, School of Chemical Sciences, Central University of Karnataka, Kalaburagi 585367 Karnataka, India*

Shamasoddin Shekh − *Department of Chemistry, School of Chemical Sciences, Central University of Karnataka, Kalaburagi 585367 Karnataka, India*

Pooja Dhurjad − *Department of Pharmaceutical Analysis, National Institute of Pharmaceutical Education and Research (NIPER), Hyderabad 500037 Telangana, India*

Ashwini Dolle − *Department of Chemistry, School of Chemical Sciences, Central University of Karnataka, Kalaburagi 585367 Karnataka, India*

Sreepriya Kakkat − *Department of Chemistry, School of Chemical Sciences, Central University of Karnataka, Kalaburagi 585367 Karnataka, India*

Vishwajyothi − *Department of Chemistry, School of Chemical Sciences, Central University of Karnataka, Kalaburagi 585367 Karnataka, India*

Marimuthu Vijayasarathy − *National Centre for Biological Sciences (NCBS), Bangalore 560065, India*

Rajesh Sonti − *Department of Pharmaceutical Analysis, National Institute of Pharmaceutical Education and Research (NIPER), Hyderabad 500037 Telangana, India*

Complete contact information is available at: https://pubs.acs.org/10.1021/acsomega.4c01028

Author Contributions

K.H.G. and S.D. conceived the study. S.D. performed the experiments and analyzed the data. S.S. and A.D. assisted in experiments. S.K. and V. assisted in the conformational analysis of redox proteins. M.V. conducted venom duct transcriptome analysis. P.D. and R.S. performed mass spectrometry experiments.

Funding

This work was supported by a DST-SERB-ECR research grant from the Government of India. S.D. and A.D. received a Junior Research Fellowship (JRF) from the Council of Scientific & Industrial Research (CSIR), India. S.S. acknowledges financial support from the Directorate of Minorities Welfare, Government of Karnataka. K.H.G. acknowledges the financial support of the DST-SERB-ECR research grant (ECR/2016/000028). R.S. acknowledges the financial support of the DST-SERB-ECR research grant (SRG/2021/002088).

Notes

The authors declare no competing financial interest.

■ ACKNOWLEDGMENTS

The authors acknowledge Prof. P. Balaram for continuously supporting the research work on conus venom peptides with gene transcripts, useful inputs, and guidance. The authors also acknowledge technical support and troubleshooting of DFT calculations and tools from the Schrodinger team, Dr. Prithesh Bhat, and Dr. Sudharshan Pandyan. S.D. and A.D. acknowledge the financial support of the Junior Research Fellowship (JRF) from the Council of Scientific & Industrial Research (CSIR), India. S.S. acknowledges the financial support from the Directorate of Minorities Welfare, Govt of Karnataka. K.H.G. and R.S. acknowledge the financial support of the DST-SERB-ECR research grant. S.D. and K.H.G. acknowledge the support of Ms. Spoorti MM, Department of Chemistry, CUK and Ms. Silpa Behera, Department of Chemistry, CUK.

■ DEDICATION

This article is dedicated to Prof. P. Balaram, National Centre for Biological Sciences (NCBS), Bangalore, as part of the celebration of his 75th birthday.

■ ABBREVIATIONS

Li520:conopeptide from *C. lividus* with mass 520 Da
Grx506:active-site tetrapeptide motif of glutaredoxin with mass 506 Da
Hyp:4-trans-hydroxyproline
PDI:protein disulfide isomerase
DFT:density functional theory

■ REFERENCES

(1) Olivera, B. M. Conus Venom Peptides: Reflections from the Biology of Clades and Species. *Annu. Rev. Ecol. Syst.* **2002**, *33*, 25−47.

(2) Olivera, B. M.; Seger, J.; Horvath, M. P.; Fedosov, A. E. Prey-Capture Strategies of Fish-Hunting Cone Snails: Behavior, Neurobiology and Evolution. *Brain Behav. Evol.* **2015**, *86*, 58−74.

(3) Olivera, B. M.; Gray, W. R.; Zeikus, R.; McIntosh, J. M.; Varga, J.; Rivier, J.; et al. Peptide neurotoxins from fish-hunting cone snails. *Science* **1985**, *230*, 1338−1343.

(4) Jin, A.-H.; Dutertre, S.; Dutt, M.; Lavergne, V.; Jones, A.; Lewis, R. J.; Alewood, P. F. Transcriptomic-Proteomic Correlation in the Predation-Evoked Venom of the Cone Snail, *Conus imperialis*. *Mar. Drugs* **2019**, *17* (3), 177.

(5) Terlau, H.; Olivera, B. M. Conus venoms: a rich source of novel ion channel-targeted peptides. *Physiol. Rev.* **2004**, *84*, 41−68.

(6) Olivera, B. M. E.E. Just Lecture, 1996. Conus venom peptides, receptor and ion channel targets, and drug design: 50 million years of neuropharmacology. *Mol. Biol. Cell* **1997**, *8*, 2101−2109.

(7) Lewis, R. J.; Garcia, M. L. Therapeutic potential of venom peptides. *Nat. Rev. Drug Discovery* **2003**, *2*, 790−802.

(8) Nguyen, L. T. T.; Craik, D. J.; Kaas, Q. Bibliometric Review of the Literature on Cone Snail Peptide Toxins from 2000 to 2022. *Mar. Drugs* **2023**, *21*, 154.
(9) Bulaj, G.; Olivera, B. M. Folding of conotoxins: formation of the native disulfide bridges during chemical synthesis and biosynthesis of Conus peptides. *Antioxid. Redox Signaling* **2008**, *10*, 141−155.
(10) Buczek, O.; Bulaj, G.; Olivera, B. M. Conotoxins and the posttranslational modification of secreted gene products. *Cell. Mol. Life Sci.* **2005**, *62*, 3067−3079.
(11) Bulaj, G.; Buczek, O.; Goodsell, I.; Jimenez, E. C.; Kranski, J.; Nielsen, J. S.; et al. Efficient oxidative folding of conotoxins and the radiation of venomous cone snails. *Proc. Natl. Acad. Sci. U.S.A.* **2003**, *100*, 14562−14568.
(12) Safavi-Hemami, H.; Li, Q.; Jackson, R. L.; Song, A. S.; Boomsma, W.; Bandyopadhyay, P. K.; et al. Rapid expansion of the protein disulfide isomerase gene family facilitates the folding of venom peptides. *Proc. Natl. Acad. Sci. U.S.A.* **2016**, *113*, 3227−3232.
(13) Gowd, K. H.; Krishnan, K. S.; Balaram, P. Identification of *Conus amadis* disulfide isomerase: minimum sequence length of peptide fragments necessary for protein annotation. *Mol. BioSyst.* **2007**, *3*, 554−566.
(14) Wang, L.; Wang, X.; Ren, Z.; Tang, W.; Zou, Q.; Wang, J.; et al. Oxidative Folding of Conopeptides Modified by Conus Protein Disulfide Isomerase. *Protein J.* **2017**, *36*, 407−416.
(15) Figueroa-Montiel, A.; Ramos, M. A.; Mares, R. E.; Dueñas, S.; Pimienta, G.; Ortiz, E.; et al. In Silico Identification of Protein Disulfide Isomerase Gene Families in the De Novo Assembled Transcriptomes of Four Different Species of the Genus Conus. *PLoS One* **2016**, *11*, No. e0148390.
(16) Safavi-Hemami, H.; Bulaj, G.; Olivera, B. M.; Williamson, N. A.; Purcell, A. W. Identification of Conus peptidylprolyl cis-trans isomerases (PPIases) and assessment of their role in the oxidative folding of conotoxins. *J. Biol. Chem.* **2010**, *285*, 12735−12746.
(17) Lluisma, A. O.; Milash, B. A.; Moore, B.; Olivera, B. M.; Bandyopadhyay, P. K. Novel venom peptides from the cone snail Conus pulicarius discovered through next-generation sequencing of its venom duct transcriptome. *Mar. Genomics* **2012**, *5*, 43−51.
(18) Vijayasarathy, M.; Balaram, P. Cone snail prolyl-4-hydroxylase α-subunit sequences derived from transcriptomic data and mass spectrometric analysis of variable proline hydroxylation in *C. amadis* venom. *J. Proteomics* **2019**, *194*, 37−48.
(19) Safavi-Hemami, H.; Gorasia, D. G.; Steiner, A. M.; Williamson, N. A.; Karas, J. A.; Gajewiak, J.; et al. Modulation of conotoxin structure and function is achieved through a multienzyme complex in the venom glands of cone snails. *J. Biol. Chem.* **2012**, *287*, 34288−34303.
(20) Dolle, A.; Vijayasarathy, M.; Shekh, S.; Hunashal, Y.; Reddy, K. K. A.; Prakash, S.; et al. The Redox-Active Conopeptide Derived from the Venom Duct Transcriptome of *Conus lividus* Assists in the Oxidative Folding of Conotoxin. *Biochemistry* **2021**, *60*, 1299−1311.
(21) Shekh, S.; Dhurjad, P.; Vijayasarathy, M.; Dolle, A.; Dhannura, S.; Sahoo, D. K.; et al. Oxidative Folding Catalysts of Conotoxins Derived from the Venom Duct Transcriptome of *C. frigidus* and *C. amadis*. *Biochemistry* **2023**, *62*, 3061−3075.
(22) Olivera, B. M.; Miljanich, G. P.; Ramachandran, J.; Adams, M. E. Calcium channel diversity and neurotransmitter release: the omega-conotoxins and omega-agatoxins. *Annu. Rev. Biochem.* **1994**, *63*, 823−867.
(23) McIntosh, J. M.; Santos, A. D.; Olivera, B. M. Conus peptides targeted to specific nicotinic acetylcholine receptor subtypes. *Annu. Rev. Biochem.* **1999**, *68*, 59−88.
(24) Jacob, R. B.; McDougal, O. M. The M-superfamily of conotoxins: a review. *Cell. Mol. Life Sci.* **2010**, *67*, 17−27.
(25) Green, B. R.; Olivera, B. M. Venom Peptides From Cone Snails: Pharmacological Probes for Voltage-Gated Sodium Channels. *Curr. Top Membr.* **2016**, *78*, 65−86.
(26) Sonti, R.; Gowd, K. H.; Rao, K. N. S.; Ragothama, S.; Rodriguez, A.; Perez, J. J.; Balaram, P. Conformational diversity in contryphans from Conus venom: cis-trans isomerisation and aromatic/proline interactions in the 23-membered ring of a 7-residue peptide disulfide loop. *Chem. - Eur. J.* **2013**, *19*, 15175−15189.
(27) Sonti, R.; Rao, K. N. S.; Chidanand, S.; Gowd, K. H.; Raghothama, S.; Balaram, P. Conformational analysis of a 20-membered cyclic peptide disulfide from Conus virgo with a WPW segment: evidence for an aromatic-proline sandwich. *Chem. - Eur. J.* **2014**, *20*, 5075−5086.
(28) Kompella, S. N.; Hung, A.; Clark, R. J.; Marí, F.; Adams, D. J. Alanine scan of α-conotoxin RegIIA reveals a selective $\alpha3\beta4$ nicotinic acetylcholine receptor antagonist. *J. Biol. Chem.* **2015**, *290*, 1039−1048.
(29) Xu, P.; Zhang, P.; Zhu, X.; Wu, Y.; Harvey, P. J.; Kaas, Q.; et al. Structure-Activity Relationships of Alanine Scan Mutants αO-Conotoxins GeXIVA[1,2] and GeXIVA[1,4]. *J. Med. Chem.* **2023**, *66*, 10092−10107.
(30) Cabrele, C.; Fiori, S.; Pegoraro, S.; Moroder, L. Redox-active cyclic bis(cysteinyl)peptides as catalysts for in vitro oxidative protein folding. *Chem. Biol.* **2002**, *9*, 731−740.
(31) Chambers, J. E.; Tavender, T. J.; Oka, O. B. V.; Warwood, S.; Knight, D.; Bulleid, N. J. The reduction potential of the active site disulfides of human protein disulfide isomerase limits oxidation of the enzyme by Ero1α. *J. Biol. Chem.* **2010**, *285*, 29200−29207.
(32) Govindu, P. C. V.; Mohanan, A.; Dolle, A.; Gowd, K. H. Conformations of cysteine disulfides of peptide toxins: Advantage of differentiating forward and reverse asymmetric disulfide conformers. *J. Biomol. Struct. Dyn.* **2019**, *37*, 2017−2029.
(33) Reddy, K. K. A.; Jayashree, M.; Govindu, P. C. V.; Gowd, K. H. Ligand-induced transition in conformations of vicinal cysteine disulfides in proteins. *Proteins* **2021**, *89*, 599−613.
(34) Sahoo, D. K.; Mohanty, P.; Biswal, H. S.; Gowd, K. H. Conformers influence on UV-absorbance of avobenzone. *J. Photochem. Photobiol., A* **2024**, *453*, No. 115671.
(35) Hennecke, J.; Sillen, A.; Huber-Wunderlich, M.; Engelborghs, Y.; Glockshuber, R. Quenching of Tryptophan Fluorescence by the Active-Site Disulfide Bridge in the DsbA Protein from *Escherichia coli*. *Biochemistry* **1997**, *36*, 6391−6400.
(36) Wunderlich, M.; Otto, A.; Seckler, R.; Glockshuber, R. Bacterial protein disulfide isomerase: efficient catalysis of oxidative protein folding at acidic pH. *Biochemistry* **1993**, *32*, 12251−12256.
(37) Guez, V.; Roux, P.; Navon, A.; Goldberg, M. E. Role of individual disulfide bonds in hen lysozyme early folding steps. *Protein Sci.* **2002**, *11*, 1136−1151.
(38) Kersteen, E. A.; Barrows, S. R.; Raines, R. T. Catalysis of protein disulfide bond isomerization in a homogeneous substrate. *Biochemistry* **2005**, *44*, 12168−12178.
(39) Schmidt, B.; Ho, L.; Hogg, P. J. Allosteric disulfide bonds. *Biochemistry* **2006**, *45*, 7429−7433.
(40) Schmidt, B.; Hogg, P. J. Search for allosteric disulfide bonds in NMR structures. *BMC Struct. Biol.* **2007**, *7*, 49.
(41) Marques, J. R. F.; da Fonseca, R. R.; Drury, B.; Melo, A. Conformational characterization of disulfide bonds: a tool for protein classification. *J. Theor. Biol.* **2010**, *267*, 388−395.
(42) Freedman, R. B.; Hirst, T. R.; Tuite, M. F. Protein disulphide isomerase: building bridges in protein folding. *Trends Biochem. Sci.* **1994**, *19*, 331−336.
(43) Holmgren, A. Thioredoxin and glutaredoxin systems. *J. Biol. Chem.* **1989**, *264*, 13963−13966.
(44) Wang, P. F.; Veine, D. M.; Ahn, S. H.; Williams, C. H. J. A stable mixed disulfide between thioredoxin reductase and its substrate, thioredoxin: preparation and characterization. *Biochemistry* **1996**, *35*, 4812−4819.
(45) Kaas, Q.; Yu, R.; Jin, A.-H.; Dutertre, S.; Craik, D. J. ConoServer: updated content, knowledge, and discovery tools in the conopeptide database. *Nucleic Acids Res.* **2012**, *40*, D325−D330.
(46) Pardos-Blas, J. R.; Tenorio, M. J.; Galindo, J. C. G.; Zardoya, R. Comparative Venomics of the Cryptic Cone Snail Species *Virroconus ebraeus* and *Virroconus judaeus*. *Mar. Drugs* **2022**, *20*, 149.
(47) Dutertre, S.; Jin, A.; Kaas, Q.; Jones, A.; Alewood, P. F.; Lewis, R. J. Deep venomics reveals the mechanism for expanded peptide

https://doi.org/10.1021/acsomega.4c01028
ACS Omega 2024, 9, 37596−37609

diversity in cone snail venom. *Mol. Cell. Proteomics* **2013**, *12*, 312−329.
(48) Robinson, S. D.; Safavi-Hemami, H.; McIntosh, L. D.; Purcell, A. W.; Norton, R. S.; Papenfuss, A. T. Diversity of conotoxin gene superfamilies in the venomous snail, *Conus victoriae*. *PLoS One* **2014**, *9*, No. e87648.
(49) Abalde, S.; Tenorio, M. J.; Afonso, C. M. L.; Zardoya, R. Conotoxin Diversity in *Chelyconus ermineus* (Born, 1778) and the Convergent Origin of Piscivory in the Atlantic and Indo-Pacific Cones. *Genome Biol. Evol.* **2018**, *10*, 2643−2662.
(50) Rajaian Pushpabai, R.; Wilson Alphonse, C. R.; Mani, R.; Arun Apte, D.; Franklin, J. B. Diversity of Conopeptides and Conoenzymes from the Venom Duct of the Marine Cone Snail *Conus bayani* as Determined from Transcriptomic and Proteomic Analyses. *Mar. Drugs* **2021**, *19*, 202.
(51) Kaas, Q.; Westermann, J.-C.; Halai, R.; Wang, C. K. L.; Craik, D. J. ConoServer, a database for conopeptide sequences and structures. *Bioinformatics* **2008**, *24*, 445−446.
(52) Han, Y.; Huang, F.; Jiang, H.; Liu, L.; Wang, Q.; Wang, Y.; et al. Purification and structural characterization of a D-amino acid-containing conopeptide, conomarphin, from *Conus marmoreus*. *FEBS J.* **2008**, *275*, 1976−1987.
(53) Lavergne, V.; Dutertre, S.; Jin, A.; Lewis, R. J.; Taft, R. J.; Alewood, P. F. Systematic interrogation of the *Conus marmoreus* venom duct transcriptome with ConoSorter reveals 158 novel conotoxins and 13 new gene superfamilies. *BMC Genomics* **2013**, *14*, 708.
(54) Vijayasarathy, M.; Basheer, S. M.; Franklin, J. B.; Balaram, P. Contryphan Genes and Mature Peptides in the Venom of Nine Cone Snail Species by Transcriptomic and Mass Spectrometric Analysis. *J. Proteome Res.* **2017**, *16*, 763−772.
(55) Fedosov, A.; Tucci, C. F.; Kantor, Y.; Farhat, S.; Puillandre, N. Collaborative Expression: Transcriptomics of Conus virgo Suggests Contribution of Multiple Secretory Glands to Venom Production. *J. Mol. Evol.* **2023**, *91*, 837−853.
(56) Safavi-Hemami, H.; Hu, H.; Gorasia, D. G.; Bandyopadhyay, P. K.; Veith, P. D.; Young, N. D.; et al. Combined proteomic and transcriptomic interrogation of the venom gland of Conus geographus uncovers novel components and functional compartmentalization. *Mol. Cell. Proteomics* **2014**, *13*, 938−953.

https://doi.org/10.1021/acsomega.4c01028
ACS Omega 2024, 9, 37596−37609